JOURNAL OF CATALYSIS 54, 405–413 (1978)

Ion-Exchanged Ultrastable Y Zeolites

II. Alkaline Earth-Exchanged Zeolites

J. SCHERZER* AND J. L. BASS

W. R. Grace & Co., Davison Chemical Division, Washington Research Center, Columbia, Maryland 21044

Received December 20, 1977; revised May 30, 1978

The preparation and structural characteristics of alkaline earth-exchanged ultrastable Y zeolites (M^{II}, H-USY) are described and discussed. M^{II}, H-USY zeolites were prepared at different exchange pH. These materials have good crystallinity and stability. Their thermal stability decreases with increasing ionic radius of the alkaline earth metal. The Brønsted acidity shows a similar trend. However, the affinity for zeolitic sites increases with ionic radius. The infrared spectra of M^{II}, H-USY zeolites in the OH stretching region and in the framework vibrational region are described. Pyridine adsorption experiments indicate the presence of both Brønsted and Lewis acidity. Steaming results in decrease of Brønsted acidity, shrinking in unit cell size, further dealumination of the zeolitic framework, and cationic migration.

INTRODUCTION

Ultrastable Y zeolites (USY) react with metal salt solutions of different acidity, resulting in metal–hydrogen-exchanged USY zeolites (M, H-USY). The formation and properties of lanthanum–hydrogen-exchanged USY zeolites have been previously described (*1*). In the present paper, we describe the preparation and structural characteristics of alkaline earth-exchanged USY zeolites.

EXPERIMENTAL METHODS

A. Materials

The starting material used in these preparations was a low-soda, ultrastable Y zeolite, type II, prepared by the method described in (*2*) or (*3*). The zeolite had a SiO_2/Al_2O_3 mole ratio of 4.85, 0.2 wt% Na_2O and a BET surface area of 763 m^2/g. One group of materials was prepared by exchanging the USY zeolite twice with a solution of metal nitrate at 90°C for 30 min, using 0.2 mole of alkaline earth nitrate per 100 g of zeolite in each exchange. The pH of the slurry was left unadjusted and varied between 4.0 and 4.3. Another group of materials was prepared by treating the USY zeolite only once with the metal nitrate solution and carrying out the exchange at an adjusted pH of 2.5 under the same conditions. The metal–hydrogen-exchanged zeolites were washed nitrate free and dried at 110°C.

B. Instrumentation and Infrared Measurements

A Beckman IR-12 spectrophotometer was used for the infrared measurements. The method used is the same as previously described (*1*). Spectra were recorded for the hydroxyl region (3000–4000 cm^{-1}) and zeolite framework region (400–1300

* Present address: Filtrol Co., 3250 E. Washington Boulevard, Los Angeles, California 90023.

0021-9517/78/0543-0405$02.00/0

cm^{-1}). The spectra in the OH region and of adsorbed pyridine were obtained with self-supporting pellets. Reflectance spectra were recorded for the framework region, using a Wilks Model 38 attenuated total reflection (ATR) unit. The spectra of adsorbed pyridine were recorded in the 1300 to 1800 cm^{-1} region, after outgassing the sample at 200°. The effect of pyridine adsorption upon the OH stretching region of the spectra was measured under similar conditions. Intensities of the bands attributed to Brønsted and Lewis acidities were obtained by measuring the peak absorbance and normalizing to the optical thickness of the sample.

Unit cell size and surface area measurements were done by conventional methods, using a Norelco powder diffractometer and Aminco Adsorptomat, respectively. The BET method was used for surface area measurements. Steaming was done in a tubular furnace with 100% steam at 540° and atmospheric pressure.

RESULTS

Analytical data for M^{II}, H-USY zeolites (M^{II} = Mg, Ca, Sr, Ba) are listed in Table 1, along with data for the USY zeolite used in these preparations. The data show that under constant exchange conditions, the metal content of the zeolite increases with the atomic weight and radius of the alkaline earth metal. For a given cation, the decrease in exchange pH from about 4 to 2.5 leads to a decrease in metal input as well as to an increase in SiO_2/Al_2O_3 ratio in the zeolite.

Unit cell size data for M^{II}, H-USY zeolites measured before and after steaming, are also shown in Table 1.

The infrared spectra in the OH region of M^{II}, H-USY zeolites before and after steaming are presented in Fig. 1. The fresh zeolites, prepared at exchange pH $\geq$ 4, show the following bands in their spectra: near 3750, 3690, 3635, and 3565 cm^{-1}. Steaming results in almost total disappearance of the bands in the 3635- and 3565-cm^{-1} region and reveals the presence of a band at about 3600 cm^{-1}. All these bands are characteristic for ultrastable Y zeolites (*3*, *4*).

The spectra of M^{II}, H-USY prepared at an exchange pH 2.5 are similar to the spectra of zeolites prepared at pH $\geq$ 4.

TABLE 1

Composition and Properties of M^{II}, H-USY Zeolites (M^{II} = Mg, Ca, Sr, Ba)

No.	Compound	Treat pH	$M^{II}O$ (wt%)	$SiO_2/Al_2O_3/M^{II}O$ (mole ratio)	SA (m^2/g) after 540°/2 hr	Unit cell size (Å) after		Peak height[a] loss at 900°/2 hr (%)
						540°/3 hr	Steam 540°/3 hr	
1	Mg, H-USY	4.0–4.3	2.12	4.8/1/0.21	700	24.52	24.43	17
2	Ca, H-USY	4.0–4.3	2.98	4.8/1/0.214	692	24.53	24.49	24
3	Sr, H-USY	4.0–4.3	5.84	4.8/1/0.23	670	24.53	24.48	32
4	Ba, H-USY	4.0–4.3	9.04	4.8/1/0.25	645	24.52	24.45	58
5	Mg, H-USY	2.5	0.53	6.2/1/0.06	703	24.48	24.35	13
6	Ca, H-USY	2.5	1.03	6.2/1/0.09	685	24.49	24.39	16
7	Sr, H-USY	2.5	2.21	6.5/1/0.11	661	24.49	24.40	26
8	Ba, H-USY	2.5	4.26	6.6/1/0.14	640	24.46	24.36	37
9	USY	—	—	4.8/1/0	721	24.48	24.33	7

[a] Expressed as percentage of peak height at $2\theta = 23.8°$ in X-ray diffractogram of corresponding compound calcined at 540°/2 hr.

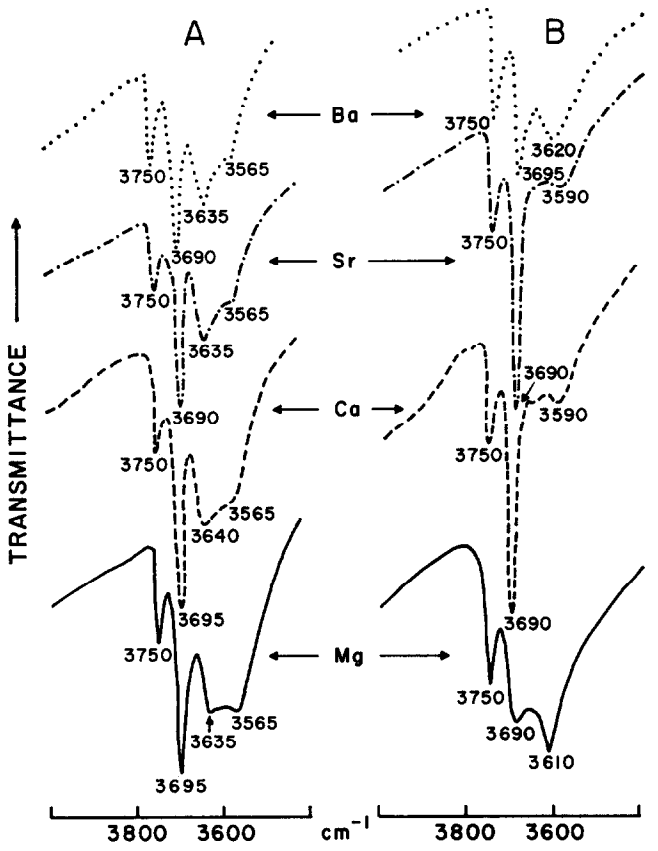

FIG. 1. Hydroxyl stretching region of M^{II}, H-USY zeolites (M^{II} = Mg, Ca, Sr, Ba) exchanged at pH $\geq$ 4. (A) Samples outgassed at 500°/1 hr; (B) samples steamed at 540°/3 hr.

Figure 2 illustrates the effect of pyridine adsorption on OH bands in the spectra of fresh and steamed M^{II}, H-USY (M^{II} = Ca, Ba). The spectra of fresh M^{II}, H-USY reveal the presence of a band in the 3600-cm^{-1} region that is otherwise masked by the bands in the 3635- and 3565-cm^{-1} regions in the absence of pyridine. In the case of steamed M^{II}, H-USY pyridine adsorption has little effect upon the OH region of the spectra, except for weakening the band at 3690 cm^{-1}.

Figure 3 shows the spectra of pyridine adsorbed on fresh and steamed Mg, H-USY.

The framework vibrational spectra for Mg, H-USY (exchange pH 4.0) before and after steaming at 540° for 3 hr are shown in Fig. 4.

The variation in the position of the (Si, Al)–O asymmetric stretching band as a result of steaming of M^{II}, H-USY zeolites is plotted in Fig. 5.

Figure 6 correlates the intensity of the band at 1545 cm^{-1} in the spectra of pyridine adsorbed on M^{II}, H-USY and the desorption temperature of pyridine. The data show a decrease in the intensity of the band with increasing desorption temperature, with Mg, H-USY having the strongest and Ba, H-USY the weakest band at 1545 cm^{-1}.

In Fig. 7, the intensities of the Brønsted and Lewis acidity bands in the spectra of pyridine adsorbed on fresh M^{II}, H-USY are plotted against the ionic radius of the alkaline earth cation.

DISCUSSION

A. *Structural Characterization*

By treating an ultrastable Y zeolite with acidic solutions of metal salts, reactions take place involving metal–hydrogen ion exchange and aluminum solubilization (nonframework and framework aluminum). The type and extent of these reactions depends upon the cationic species in solution and the exchange conditions—pH, concentration, temperature, *et al.*

By exchanging ultrastable Y zeolite with alkaline earth cations at pH $\geq$ 4, the predominant reaction is the exchange of zeolitic protons for metal cations. The increase in the number of metal cations exchanged into the zeolite with increasing atomic weight and radius—under otherwise constant exchange conditions—is related to the corresponding increase in affinity for zeolitic sites. A similar affinity sequence has been observed in the study of ion-exchange equilibria between alkaline earth cations and NaY zeolites (*5*). Such an affinity sequence has been related to the decrease in hydration energies with increasing ionic radii in the alkaline earth series. This results in lower energy barriers to diffusion into the zeolite. Standard enthalpy measurements for exchange reactions of alkaline earth cations into NaX and NaY zeolites have shown that barium ions are the most preferred (*6*). Our data

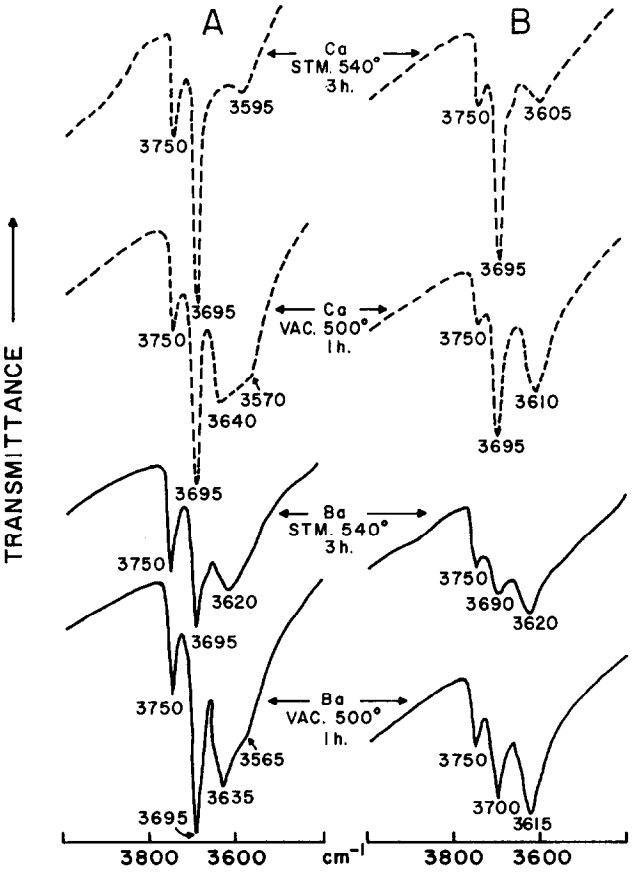

FIG. 2. Effect of pyridine adsorption on OH stretching region of Ca, H-USY and Ba, H-USY zeolites, both fresh and steamed. (A) Before pyridine adsorption; (B) after pyridine adsorption.

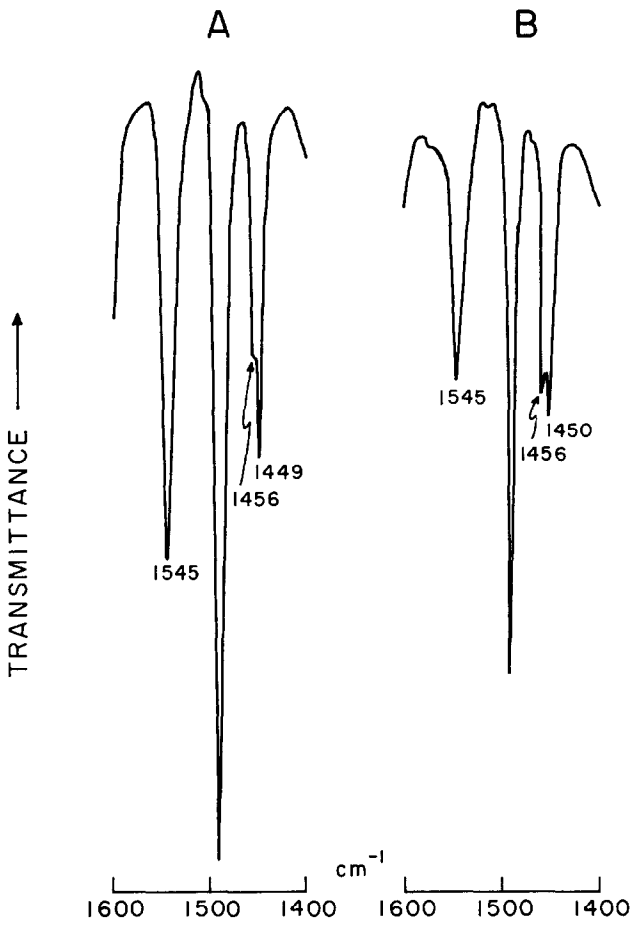

FIG. 3. Spectra of pyridine adsorbed on Mg, H-USY zeolite before and after steaming. (A) Before steaming; (B) after steaming.

suggest that such an interpretation applies also to the exchange of USY zeolites with alkaline earth cations.

B. Effect of Exchange pH

The decrease in metal exchange into the zeolite at the lower pH of 2.5 is due to increased competition for exchange sites by the hydronium ions in solution. Moreover, the lower exchange pH also results in partial aluminum leaching, as reflected by the higher SiO_2/Al_2O_3 ratio in the zeolite. It is primarily nonframework aluminum that is leached under these conditions, as indicated by the identical position of the (Si, Al–O) asymmetric stretching band in the spectra of M^{II}, H-USY prepared at the high and low pH. The Sr and Ba zeolites exchanged at pH 2.5 have higher SiO_2/Al_2O_3 ratios and higher alkaline earth contents that the corresponding Mg and Ca zeolites (see Table 1). This is due to additional nonframework aluminum exchange by Sr^{2+} and Ba^{2+}, as a result of the higher affinity of these ions for exchange sites.

C. Thermal Stability of M^{II}, H-USY

The crystallinity of these zeolites is high, as reflected by their high surface area following outgassing at 540°. The decrease in surface area with increasing

cationic radius in M^{II}, H-USY zeolites prepared under otherwise identical conditions is due to the increase in the volume occupied by the cationic species. Their thermal stability decreases with increasing cationic radius, as shown by the relative peak height loss after calcination at 900°. The decrease in stability is most likely related to the increase in basicity of the cation. This brings the alkaline earth-exchanged zeolite closer to the alkaline metal-exchanged forms which have lower thermal stability (*7*). Differences in cationic distribution will also effect the stability of the zeolites (*vide infra*). For a given alkaline earth cation, an increase in the metal content of the zeolite results in a decrease in thermal stability. The metal exchanged forms are generally less stable than the initial USY zeolites.

D. Effect of Hydrothermal Treatment

It has been shown (*3*, *8–14*) that hydrothermal treatment of faujasite-type zeolites can lead to: (a) partial framework dealumination, resulting in the formation of nonframework aluminum species; (b) structural rearrangement in the framework, leading to the elimination of defects left by dealumination; (c) unit cell shrinking, due primarily to framework dealumination and structural rearrangement; (d) cationic migration; (e) decline in acidity and ion-exchange capability, as a result of dehydroxylation and structural changes in the framework. Such modifications are more pronounced in the NH_4^+ (or H^+)-exchanged form of the zeolite and, to a lesser extent, in the metal–ammonia (or metal–hydrogen)-exchanged forms.

These processes take place during the

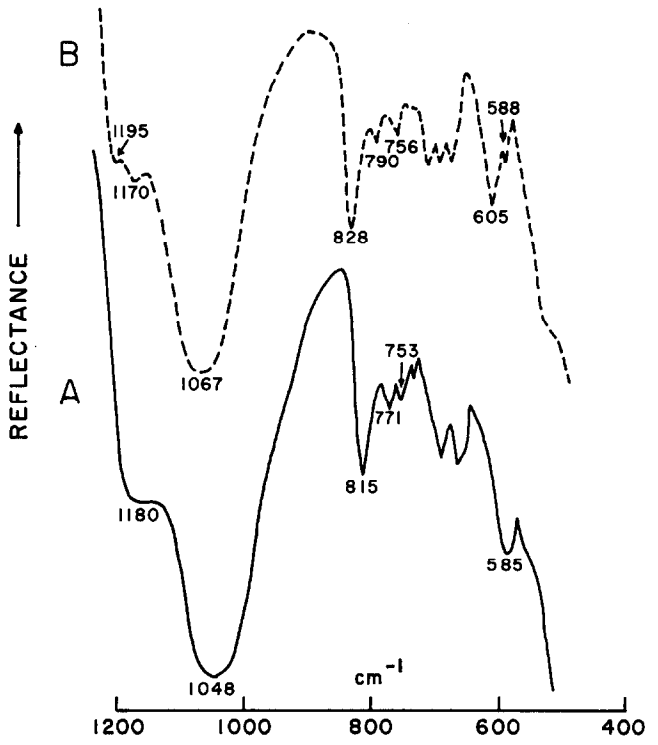

FIG. 4. Framework vibrational spectra of Mg, H-USY zeolite before and after steaming. (A) Before steaming; (B) after steaming.

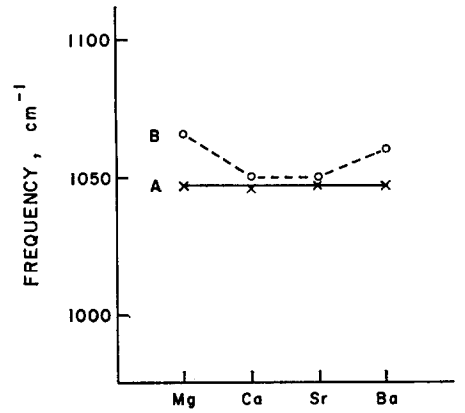

FIG. 5. Position of Si, Al–O asymmetric stretching band in spectra of M^{II}, H-USY zeolites before and after steaming. (A) Before streaming; (B) after steaming.

high-temperature steaming required for the preparation of ultrastable Y zeolites. Additional dealumination and unit cell shrinking occurs during steaming of alkaline earth-exchanged ultrastable zeolites, together with migration of the metal cations.

E. Cationic Migration and Unit Cell Size

Structural studies of alkaline earth-exchanged faujasite-type zeolites have shown (*15*, *16*) that prior to thermal treatment most divalent ions occupy sites in the supercage, where they occur in hydrated form. The occupancy of sites in the smaller cavities is rather small. Upon dehydration, a redistribution of cations takes place, with most or all divalent ions migrating from supercage positions into the smaller cavities through the six-member rings (*17–20*). The equilibrium concentration of alkaline earth ions diffusing through the six-member rings depends upon the hydration energies—or size of the hydrated ion—and the radius of the bare ion.

In the case of ultrastable Y zeolites, two additional factors will affect the cationic distribution in the zeolite: (a) smaller six-member rings as a result of shorter (Si, Al)–O bonds in the USY zeolites (*10*); (b) the presence of nonframework aluminum species in the sodalite cages.

Due to these factors, the migration of alkaline earth cations into the small cages during hydrothermal treatment becomes more difficult than in the corresponding Y zeolites. Moreover, as the size of the ion increases, the energy barrier to diffusion increases. Therefore, we can expect fewer Ba ions in the small cages, although the total amount of Ba ions in the zeolite is higher than that of the other alkaline earth.

Such an interpretation is in agreement

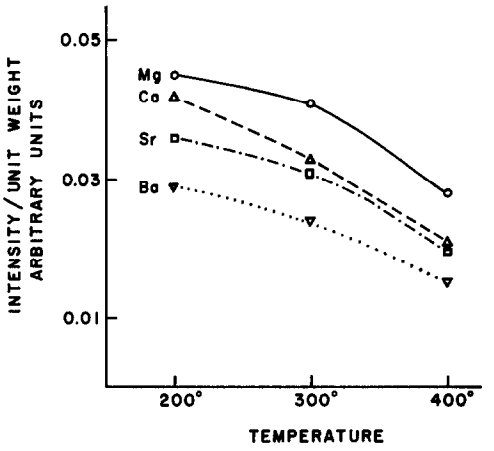

FIG. 6. Variation in intensity of 1545 cm^{-1} Brønsted acidity band with temperature.

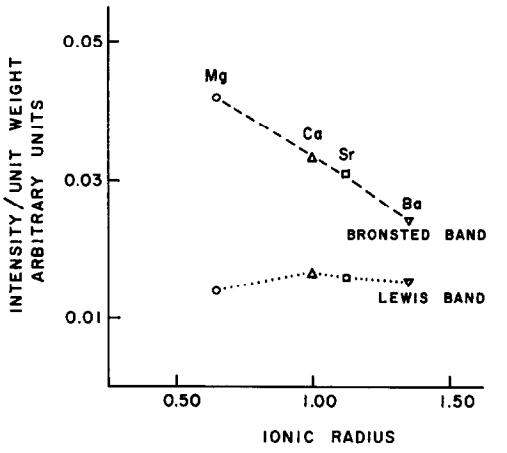

FIG. 7. Variation in intensities of Brønsted and Lewis acidity bands with ionic radius. ○, Mg; △, Ca; □, Sr; ▽, Ba.

with the unit cell sizes of hydrothermally treated M^{II}, H-USY. Under identical treatment, the degree of unit cell shrinking will depend upon the type and number of polyvalent ions in the small cages. The cations left in the supercages are less likely to affect the degree of framework shrinking. For example, in La, H-Y zeolites it was found that a decrease in La content in the sodalite cages results in stronger unit cell shrinking during steaming (*21*). In steamed M^{II}, H-USY, the unit cell size increases from Mg to Ca, but decreases from Sr to Ba (Table 1). The Ca and Sr forms have virtually the same unit cell size. This suggests that Mg, Ca, and to a certain extent Sr ions diffuse into the smaller cages during steaming. The increase in unit cell size from Mg to Ca is due primarily to the increase in ionic radius. The nearly identical unit cell sizes of the Ca and Sr forms are most likely the result of fewer Sr ions in the smaller cages. The low concentration of Ba ions in the small cages accounts for the smaller unit cell.

The small-radius M^{2+} cations have the tendency to form MOH^+ ions (*vide infra*). In the sodalite cages, these hydroxy ions can conceivably interact among themselves or with nonframework aluminum, forming complex cationic species with $-OH\cdots$ or $-O-$ bridges.

The M^{II}, H-USY zeolites prepared at exchange pH 2.5 have smaller unit cell sizes than the corresponding zeolites prepared at pH $\geq$ 4. This is due to the considerably lower concentration of alkaline earth cations in the former zeolites as well as to the removal of nonframework aluminum by the more acidic solution.

F. Framework Vibrational Spectra

Prior to steaming, the framework vibrational spectra of all M^{II}, H-USY are practically identical. Steaming at 540° results in a shift of bands to higher wave members. The shift is most obvious for the (Si–Al)–O asymmetric stretching band located in the 1000 to 1100-cm^{-1} region. The magnitude of the shift depends upon the type of cation in the zeolite. The plot in Fig. 5 shows that prior to steaming, this band has practically the same frequency for all M^{II}, H-USY zeolites. However, the spectra of steamed M^{II}, H-USY show that the strongest shift occurs for the Mg and Ba forms. Since a shift of the asymmetric stretching band to higher frequencies is indicative of an increase of the SiO/Al_2O_3 ratio in the framework, it follows that the framework of steamed Mg and Ba forms is more siliceous than that of Ca and Sr.

G. Acidity of M^{II} H-USY

The infrared spectra in the OH region (Fig. 1) show that all outgassed M^{II}, H-USY zeolites have Brønsted acidity, characterized by the band at 3635 to 3640 cm^{-1}. The concentration of Brønsted acid sites depends upon the type of alkaline earth cation. It increases with decreasing cationic radius, as reflected by the intensity of the band at 1545 cm^{-1} for adsorbed pyridine (Fig. 7). A similar observation has been made for alkaline earth Y zeolites (*22*). Such an increase in the concentration of acid sites is due to the increased polarizing power of the smaller divalent cation acting upon adjacent water molecules. It results in MOH^+ and protons attached to structural O atoms. The MOH^+ groups are nonacidic and the corresponding hydroxyls absorb at the same frequency as the nonacidic OH groups in USY—most likely at about 3690 cm^{-1} (compare OH bands of Ca and Ba form after pyridine adsorption, Fig. 2). The protons add to the Brønsted acidity of the zeolite (*22*, *23*). The decrease in Brønsted acidity with increasing cationic radius is also a result of the more advanced exchange of the initial zeolitic protons (or NH_4^+ ions) by the larger cations. The concentration of Lewis acid sites is not affected by this process and

remains practically the same for different cations.

The elimination of the OH bands at 3640 and 3565 cm^{-1} by pyridine adsorption indicates that both bands are due to acidic OH groups. The band at 3700 cm^{-1} is weakly acidic, since it interacts only partially with pyridine (Fig. 2). An increase in pyridine desorption temperature to 400° almost entirely regenerates the initial band. The band at 3600 cm^{-1} is nonacidic. These observations apply to all M^{II}, H-USY zeolites.

In the spectra of steamed zeolites, the 3640-cm^{-1} band has almost disappeared (Fig. 1). The spectra of adsorbed pyridine (Fig. 3) show that the band at 1545 cm^{-1} is still present, although it is considerably weaker. The decrease in Brønsted acidity as a result of hydrothermal treatment is obviously due to dehydroxylation and additional dealumination.

The presence of Brønsted acidity in steamed zeolites, despite the virtual absence of an absorption band at 3640 cm^{-1}, is most likely related to acidic OH groups that absorb at other frequencies (e.g., at 3690 cm^{-1}).

The band at 1450 cm^{-1}, characteristic of cation–pyridine interaction, is also weaker in the spectra of steamed zeolites. This is caused by the migration of the metal cations during steaming into the small cages, where they are inaccessible to pyridine. The Lewis acidity band at 1456 cm^{-1} is little affected by these changes.

ACKNOWLEDGMENT

The authors express their appreciation to the Davison Division of W. R. Grace & Co. for permission to publish the results of this study.

REFERENCES

1. Scherzer, J., and Bass, J. L., *J. Catal.* **46**, 100 (1977).
2. McDaniel, C. V., and Maher, P. K., *in* "Proceedings, Conference on Molecular Sieves 1967, Monograph 186. Soc. of Chem. Ind., London, 1968.
3. Scherzer, J., and Bass, J. L., *J. Catal.* **28**, 101 (1973).
4. Jacobs, P., and Uytterhoeven, J. B., *J. Catal.* **22**, 193 (1971).
5. Barrer, R. M., Davies, J. A., and Rees, L. V. C., *J. Inorg. Nucl. Chem.* **30**, 3333 (1968).
6. Sherry, H. S., *J. Phys. Chem.* **72**, 4086 (1968).
7. Breck, D. W. "Zeolite Molecular Sieves," p. 495. Wiley, New York, 1974.
8. Kerr, G. T., *J. Phys. Chem.* **71**, 4155 (1967).
9. Kerr, G. T., *J. Catal.* **15**, 200 (1969).
10. Maher, P. K., Hunter, F. D., and Scherzer, J., "Molecular Sieve Zeolites," Advances in Chemistry Series No. 101, Vol. I, p. 266. Amer. Chem. Soc., Washington, D.C., 1971.
11. Jacobs, P. A., and Uytterhoeven, J. B., *J. Chem. Soc. Faraday Trans.* **69**, 359, 373 (1973).
12. Kerr, G. T., *in* "Proceedings, 3rd International Conference on Molecular Sieves," Advances in Chemistry Series No. 121, p. 219, Amer. Chem. Soc., Washington, D.C., 1973.
13. Peri, J. B., *in* "Proceedings, 5th International Congress on Catalysis," p. 329, 1972.
14. Breck, D. W., and Seeks, G. W., *in* "Proceedings, 6th International Congress on Catalysis." 1976.
15. Bennett, J. M., and Smith, J. V., *Mater. Res. Bull.* **3**, 933 (1968).
16. Olson, D. H., and Sherry, H. S., *J. Phys. Chem.* **72**, 4095 (1968).
17. Bennett, J. M., and Smith, J. V., *Mater. Res. Bull.* **3**, 633 (1968).
18. Olson, D. H., *J. Phys. Chem.* **72**, 1400 (1968).
19. Jacobs, P. A., Cauwelaert, F. H. van, Vausant, E. F., and Uytterhoeven, J. B., *J. Chem. Soc. Faraday Trans. I* **69**, 1056 (1973).
20. Eagerton, T. A., and Stone, F. S., *Trans. Faraday Soc.* **66**, 2364 (1970).
21. Scherzer, J., Bass, J. L., and Hunter, F. D., *J. Phys. Chem.* **79**, 1194 (1975).
22. Ward, J. W., *J. Catal.* **10**, 34 (1968).
23. Eberly, P. E., *J. Phys. Chem.* **72**, 1042 (1968).